The Condition Evolution of Concrete Bridges Based on a Segmental Approach, Nondestructive Test Methods, and Deterioration Models

GUIDO ROELFSTRA
BRYAN ADEY
RADE HAJDIN
EUGEN BRÜHWILER
Swiss Federal Institute of Technology–Lausanne,
Institute of Structural Engineering and Mechanics,
MCS–Maintenance, Construction and Safety of Structures

ABSTRACT

An effective bridge management system (BMS) requires an accurate prediction of the condition deterioration of bridges and their remaining service lives. These predictions are currently based on visual inspections and comparison with older structures. These can be improved by using a segmental approach, accurate deterioration models and non-destructive testing. An on-going research project, at the Swiss Federal Institute of Technology, is evaluating the potential benefits of this approach by applying it to representative bridges of the Swiss highway system. This paper provides an overview of this approach and its application to bridges, and highlights the important findings.

INTRODUCTION

More accurate predictions of condition deterioration are required to optimize bridge management strategies. These can be attained by using a segmental approach that includes both accurate deterioration models and non-destructive testing. To demonstrate the potential of this approach, it is used to predict the life expectancies of two bridges typical of the Swiss highway bridge network. The main deterioration mechanism observed is *chloride-induced corrosion.*

Currently, the condition of bridges in many BMSs are predicted based on visual inspection of the bridges, and comparing the observed deterioration levels with those of older bridges. When bridges are relatively young, as in the Swiss highway network, there are no significant signs of deterioration. Therefore, the comparison with older bridges is difficult, making the forecast of the bridge condition almost impossible. Improved predictions of the future condition can be made by using a segmental approach, non-destructive testing and deterioration models.

CHLORIDE-INDUCED CORROSION

During cement hydration, a highly alkaline pore solution (pH 12.5–13.6) is formed in the concrete. In this alkaline environment, ordinary reinforcing steel forms a very thin oxide

film (the passive film) that protects the steel from corrosion. This passive film remains stable as long as the pore water composition remains constant. The protective film is destroyed when sufficient chloride ions (from deicing salts or from seawater) have penetrated to the reinforcement. The reinforcing steel is depassivated and thus vulnerable to corrosion attack. Once the reinforcing steel is depassivated and simultaneously in contact with both oxygen and water (humidity) metal dissolution (corrosion in the form of rust formation, loss in cross section) occurs (Figure 1).

The deterioration of concrete structures due to reinforcement corrosion can be divided into two phases (Figure 2):

(1) During the **initiation phase**, chlorides penetrate from the surface of the concrete to the reinforcement. The duration of the initiation phase is from the construction of the structure until depassivation of the reinforcing steel has occurred.

(2) During the **propagation phase**, the reinforcement actively corrodes. The duration of the propagation phase is dependent on the rate of corrosion. The propagation phase begins once the depassivation of the reinforcing steel has occurred and ends when a specified amount of section loss has occurred.

A durable concrete structure obviously has both a long initiation phase and a slow corrosion rate. Usually the conditions that provide these are similar.

Chloride penetration and corrosion are highly complex phenomena. It is however well known that they depend on parameters such as the concrete cover thickness, the porosity and permeability of surface and cover concrete, the concentration of chlorides, and the microclimatic conditions (wetting, drying) at the concrete surface. Using this knowledge and a segmental approach accurate prediction of bridge life expectancies can be made.
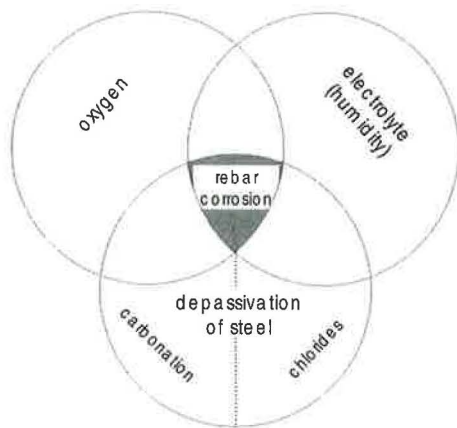
Figure 1: Conditions for steel reinforcement corrosion.
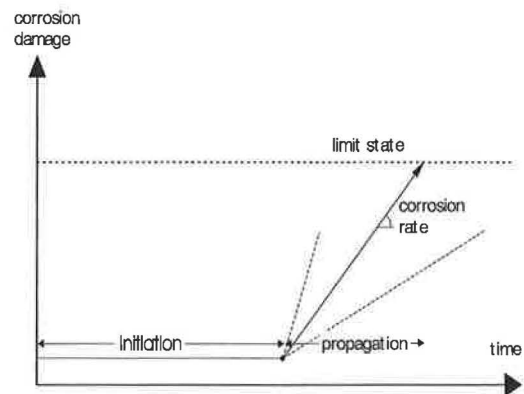
Figure 2: Development of corrosion of steel reinforcement in concrete with time.

SEGMENTAL APPROACH

Division into Segments

In the segmental approach each bridge is first divided into **elements** according to their structural role. The elements are then subdivided into **segments** with regard to structural function. For example, an element such as a girder is subdivided at least into three segments, one on each support and one in between.

      The condition of these segments, and therefore the whole bridge, can then be predicted if the active deterioration process is considered. When chloride induced corrosion is the deterioration process the three important parameters to consider are (1) exposure to chlorides and humidity, (2) concrete permeability and (3) concrete cover thickness. These parameters can be determined by visual inspections and non-destructive testing for each segment.

Exposure to Chlorides

The chloride exposure levels of the segments have an important chloride induced corrosion. In order to determine the segment exposure level, each segment was classified by exposure zone. This can be determined by visual inspection. Three exposure zones were defined and classification of typical bridge segments is shown in Table 1.

      The exposure levels of the segments change depending on weather condition. To simplify, the exposure levels were related directly to the quantity of chlorides in the water (Table 2). The chloride concentration variation for each zone simulates the mixing of chloride loaded water with non-chloride free water.

      Each year, there are three exposure levels for each exposure zone: a severe phase of three months followed by a mild phase of three months and finally a null phase of six months.

Table 1: Typical Exposure Zones

Exposure Zones	Segments

Direct (direct contact with water)	- Curb (inner side)
	- Deck (top side):
	  - Infiltration (leak)
	  - Flow
	  - Water evacuation system

Splash (splashed by passing vehicles)	- Curb (exterior side) - Pile and strut - Retaining wall
Mist (contact with mist generated by passing vehicles)	- Deck (underside) - Pile and strut - Abutment and walls - Other structure

Table 2: Chloride Content of the Water [kg/m³] for Each Exposure Level and Exposure Zone

Exposure Zone	Exposure Level		
	Severe	Mild	Null
Direct	12	6	0
Splash	6	3	0
Mist	3	1.5	0

Concrete Permeability

Concrete permeability is the most important concrete material property when modelling chloride penetration. The segments were classified into three concrete quality categories based on non-destructive permeability measurements (*1*). A normal distribution of the permeability was used to take into account the large variation observed. The relation between the measured in situ air permeability coefficient kT and the chloride diffusion coefficient D_c used in the model (Table 3) was based on experimental results (*2*).

Concrete Cover Thickness

The concrete cover thickness is important when modelling chloride induced corrosion because it affects the time to corrosion initiation. It is therefore important to determine the depth of reinforcement of each of the segments. The concrete cover thickness was determined using commercial apparatus. In general, the average depth of concrete cover was found to be close to the one specified in the design drawings and the variation was small. The standard deviation was close to 10% of the average value. In some locations, however, it was found that the concrete cover was less than 5 mm, possibly due to errors in reinforcement placement at the time of concrete pouring. These locations are indicators for the corrosion evolution for the rest of the bridge. They also enable calibration of the predictions of the deterioration model.

DETERIORATION MODEL

Once the segments were classified with respect to exposure zone, concrete permeability and the depth of the reinforcement, the deterioration of the segments due to chloride-induced corrosion was modelled in two phases: the initiation phase and the propagation phase as defined previously.

Initiation Phase

Chloride Penetration
Chloride ions penetrate into the concrete by two transport mechanisms. The first is ingress by capillary forces of water containing chlorides into the concrete. The second is

Table 3: Relationship Between in Situ Permeability Coefficient, Diffusion Coefficients and Concrete Quality

Cover concrete quality	In situ permeability coefficient kT 10^{-16} [m²]	Chloride diffusion coefficient		Water diffusion coefficient	
		D_c 10^{-12} [m²/s]	std. dev. 10^{-12} [m²/s]	D_w 10^{-12} [m²/s]	std. dev. 10^{-12} [m²/s]
Good	< 0.2	6	1.5	60	15
Average	0.2 < kT < 2.0	13	3.25	130	32.5
Bad	> 2.0	20	5	200	50

the diffusion of the chloride ions in the water already present in the concrete. Both transport mechanisms can be modelled using normal diffusion laws (*3,4*). The flux of chloride ions (J_{Cl}) can be determined by using Fick's first law:

$$J_{Cl} = -D \cdot \nabla C_f \tag{1}$$

where C_f is the concentration of free chlorides in the solution and D is the diffusion coefficient as a function of the relative humidity h_r (*3*):

$$D = D_{100\%} \cdot \left(0.05 + \frac{0.95}{1 + 3 \cdot (1 - h_r)^4} \right) \tag{2}$$

h_r can be determined by sorption and desorption isotherms (*4*), given by:

$$w = w_{sat} \cdot h_r \qquad\qquad \text{desorption} \tag{3}$$

$$w = w_{sat} \left(1.16 \cdot h_r^3 - 1.05 \cdot h_r^2 - 0.11 \cdot h_r + 1 \right) \qquad \text{sorption} \tag{4}$$

where w is the evaporable water content and w_{sat} is the maximum evaporable water content. w_{sat} for this study was 140 kg/m³.

By considering the law of mass conservation (Fick's second law):

$$\frac{\partial C_t}{\partial t} = div(J_{Cl}) \tag{5}$$

where C_t is the total chloride concentration, and that the free chloride ion concentration is given by:

$$C_f = w \cdot e \tag{6}$$

where e is the concentration of the solution, the flux of the chloride ions into the concrete becomes:

$$\frac{\partial C_t}{\partial t} = -div\left[-D_w \cdot e \frac{dw}{dx} - D_c \cdot w \frac{de}{dx} \right] \tag{7}$$

The first term represents the chloride ion transport with the water ingress by capillary forces and the second term represents the diffusion of the chloride ions within the water.

In an unsaturated concrete the total chloride concentration, C_t, is:

$$C_t = w \cdot e + (1 - w_{sat}) \cdot \gamma \cdot e \tag{8}$$

The relationship between the free and bound chloride ions is assumed as:

$$\gamma = \frac{C_f}{C_s} \tag{9}$$

In the present study γ was taken to be 0.6.

The calculation of the relative humidity, h_r, took into account the meteorological conditions in Lausanne. The meteorological conditions were simplified in the deterioration model into two blocks based on humidity levels. The first block assumed 100% humidity and consisted of the average annual number of days where more than 1 mm of rain fell. The second block assumed 60% humidity and consisted of the average annual number of days where less than 1 mm of rain fell. The meteorological data was obtained from the Swiss automatic measure network ANETZ. The chloride concentration of the water assumed in these blocks was explained previously.

The diffusion coefficients, D_c and D_w, used in the deterioration model and the relationships with cover concrete quality were calculated based on chloride penetration tests reported in the literature (5,6,7) (Table 3).

Critical Chloride Content

The modelling of the corrosion initiation time involves determing the time it takes for a corrosion-inducing concentration of chloride ions to migrate to the reinforcement level. A summary of recent research (8) showed that a wide range for the critical chloride ion content has been measured. A value of 0.4% of total chloride ions per cement weight is frequently used. This value, however, is often overly pessimistic in regard to the initiation time of corrosion for in situ conditions. The probability of corrosion initiation in this study was taken as a function of the **free** chloride ion concentration as shown in Figure 3. A normal distribution was assumed with an average value of 0.4% and a standard deviation of 0.15% for **free** chloride ion content.

The initiation probability was determined as a function of cover thickness, for each combination of exposure zone and concrete cover quality category. The 10% fractile of the initiation probability was defined as the significant value for onset of corrosion. The calculated initiation times are shown in Table 4.
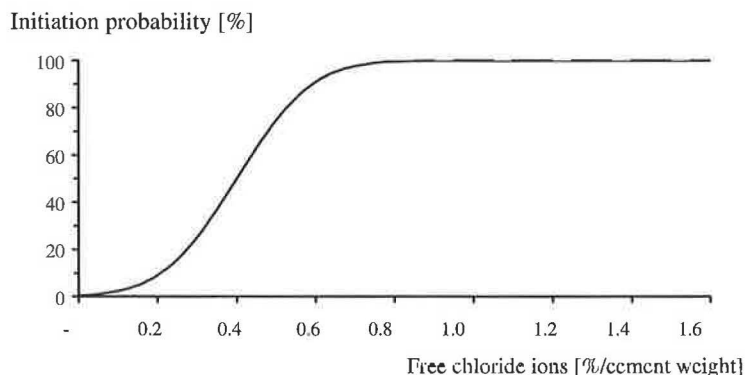
Figure 3: Corrosion initiation probability with respect to free chloride ion concentration.

Table 4: Initiation Times (years), 10% Fractile of Initiation Probability

Average concrete cover thickness [mm]	Exposure zone								
	Direct			Splash			Mist		
	Concrete quality			Concrete quality			Concrete quality		
	Poor	Aver.	Good	Poor	Aver.	Good	Poor	Aver.	Good
10	1	1	2	1	2	4	2	3	7
20	4	7	14	8	13	29	16	26	58
30	11	17	38	22	35	76	44	68	150
40	21	32	71	41	64	140	82	130	285

It can be quickly deduced from Table 4 that categorization of bridge segments by exposure zone, concrete quality and concrete cover thickness can assist in the decision making process. For example, a bridge with a 50 year design life, good quality concrete and 20 mm of concrete cover will have no corrosion in the mist zones but will have corrosion in both the splash and the direct zones. If the onset of corrosion must be prevented on the entire bridge for the entire design life of the bridge, it is the segments in the direct and splash zones that require protective actions.

Propagation Phase

Corrosion

Once the corrosion of the reinforcement is initiated, the area of the reinforcement is reduced by a corrosion speed v_{corr} (mm of material loss from reinforcement diameter per year). Many parameters influence v_{corr}, namely the chloride content, the presence of oxygen, the diffusion coefficients, the electrical resistivity of the concrete, the presence of cracks and the formation of macro-cells.

The range of observed corrosion speeds varies from 0.1 mm/year to a few mm/year including pitting corrosion (9). As this value is still uncertain, three different speeds were used in this study depending on the observed field conditions (Table 5).

Failure Scenarios

Failure mechanisms were identified for each of the bridges. Failure modes were analyzed taking into account the exposure level, the concrete quality and the concrete cover thickness of the segments. The structural safety and the deflections were estimated for the bridges by taking into consideration the condition of the segments. Two safety coefficients *n* were calculated:

Table 5: The Corrosion Speeds v_{corr} [mm/year] Used for Different Conditions

Concrete Quality	Exposure Zones		
	Direct	Splash	Mist
Good	0.5	0.1	0.1
Average	1.0	0.5	0.1
Bad	1.0	1.0	0.5

- The first calculation used material properties and load models updated according to site inspections for the investigated bridges.
- The second calculation was performed according to the Swiss design codes (*10*).

The safety coefficients are obtained by dividing the design resistance R_d by the design value of the action effect S_d. The design resistance includes the resistance factor γ_R and the design value of action effect includes all the load factors γ_g, γ_q and ψ (*10*). Values above one for the safety coefficient n indicate that the structure meets the requirements for structural safety.

CONDITION EVOLUTION OF BRIDGES

Sample Bridges

To illustrate the potential of combining the segmental approach, non-destructive test methods and deterioration models, the future condition of two sample bridges (Table 6) was predicted. The two bridge types represent a large number of highway bridges in Switzerland.
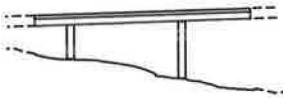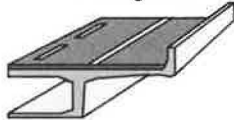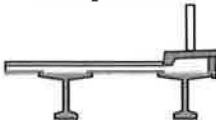
Continuous Girder Bridges

Scenario: Cantilever Failure

The investigated failure scenario of the continuous highway bridge was local failure of one of the cantilevers due to chloride-induced corrosion.

During the visual inspection of the continuous highway bridge, there was evidence of poor drainage and leaks in the waterproofing layer. Watermarks were observed indicating that water had been flowing down the side of the deck and along the underside of the cantilever. Humid zones were seen on the underside of the cantilever. The cantilever was classified in the direct exposure zone. The corrosion speed was considered to be 0.5 mm/year. Non-destructive tests showed that the bridge had good quality cover concrete but that in some local zones the inferior reinforcement was located

Table 6: Sample Bridges

Bridge	Year of Construction	Longitudinal Section	Cross Section
Continuous girder bridge	1973	continuous girder	Box girder
Strut bridge	1963	struts	Multiple beam

only a few millimeters from the concrete surface. These zones can be considered as corrosion indicators for the rest of the structure.

Because the inferior reinforcement has less concrete cover than the superior reinforcement, it was the first reinforcement to corrode. The corrosion initiation time of the transversal reinforcement had the greatest influence on the service life of the structure. Figure 4 shows the safety coefficient n with respect to time of the continuous girder bridge.

The first drop in n occurs 10 years after construction and is due to the corrosion of the inferior reinforcement. The safety coefficient calculated according to yield line analysis was reduced due to the loss of the steel cross section on the positive bending moment yield lines and the spalling that reduces the static height of the deck on the negative bending moment yield lines. The short corrosion initiation time is attributed to the small amount of concrete cover and has been observed on the bridge during the inspections. Even with the complete corrosion of the inferior reinforcement, however, the safety is still sufficient. After 25 years, the waterproofing layer is considered to be no longer effective. At this point the chloride ions started to penetrate towards the superior reinforcement (concrete cover thickness of 35 mm).

Once the superior reinforcement begins to corrode after 85 years of service life, the safety coefficient falls below acceptable limits. There are no serviceability problems due to increased deflections for this failure mechanism.

As it can be seen in Figure 4, the reduction of the safety coefficient for this bridge has plateaued today and will not decrease again for approximately 50 years. Maintenance measures should be planned such as the replacement of the waterproofing layer before the corrosion of the superior reinforcement starts.

Speed of Corrosion

For the above failure scenario, v_{corr} was taken equal to 0.5 mm/year. This was an approximation as explained in the section on corrosion. The assumption of v_{corr} has an effect
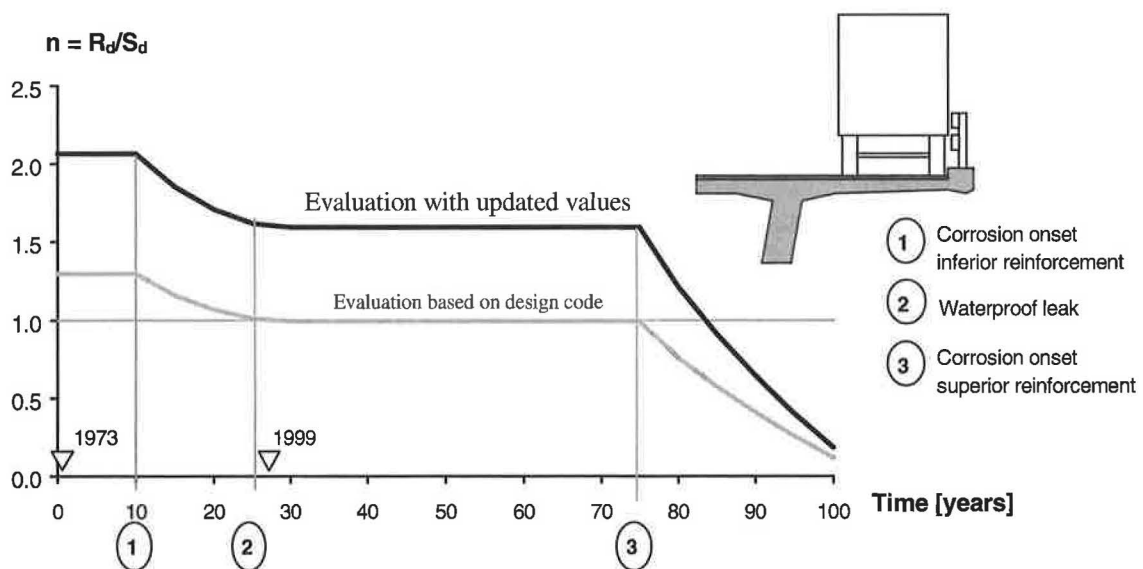
Figure 4: Safety coefficient **n**, *with respect to time, of the continuous girder bridge.*
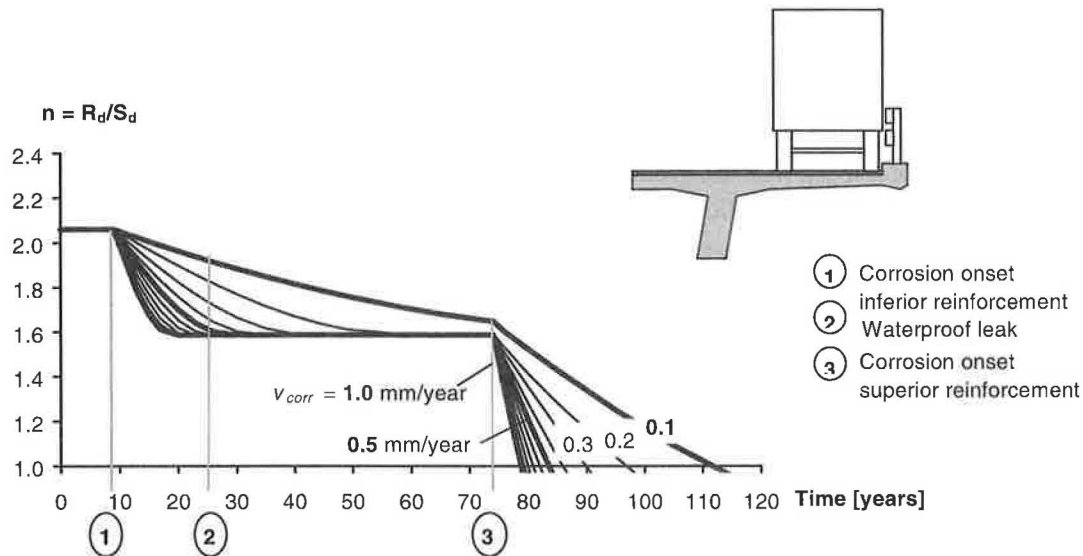
Figure 5: Local failure of the cantilever with different corrosion speeds.

on the predicted safety coefficient and the bridge life expectancy. To illustrate the effect of v_{corr} on the safety coefficient various corrosion speeds were selected and the safety factor for the continuous girder bridge was recalculated with respect to time (Figure 5). All variables were kept the same except for v_{corr}, even though in reality there is some correlation between corrosion initiation time and v_{corr}. If this correlation were included the differences in life expectancies would have been larger.

It can be seen in Figure 5 that there is little change in the service life for values of above 0.3 mm/year, which is generally the case with chloride induced corrosion (Table 5).

Corrosion Initiation Time

To show the importance of determining the corrosion initiation time, the safety coefficient for the continuous girder bridge was calculated, with different corrosion initiation times (Figure 6) but with the same corrosion speed of 0.5 mm/year. The changes in corrosion initiation time, shown in Figure 4, were calculated based on concrete covers of 25, 35 and 45 mm. The calculation of corrosion initiation time may also be affected by concrete permeability, exposure to chlorides and thickness of concrete cover.

It can be seen in Figure 6 that the corrosion initiation time has a large influence on the predicted life expectancy, which is more important than the influence of the corrosion speed (Figure 5).

Strut Bridge

The investigated failure scenario of the strut bridge was the failure of a prestressed girder (Figure 7). The visual inspection of the strut bridge indicated that the waterproofing layer was in good condition, the girders were in the mist exposure zone and the bridge. The corrosion speed was assumed to be 0.5 mm/year. The non-destructive tests showed that the girders were made of poor quality concrete and that the prestressed wires had a
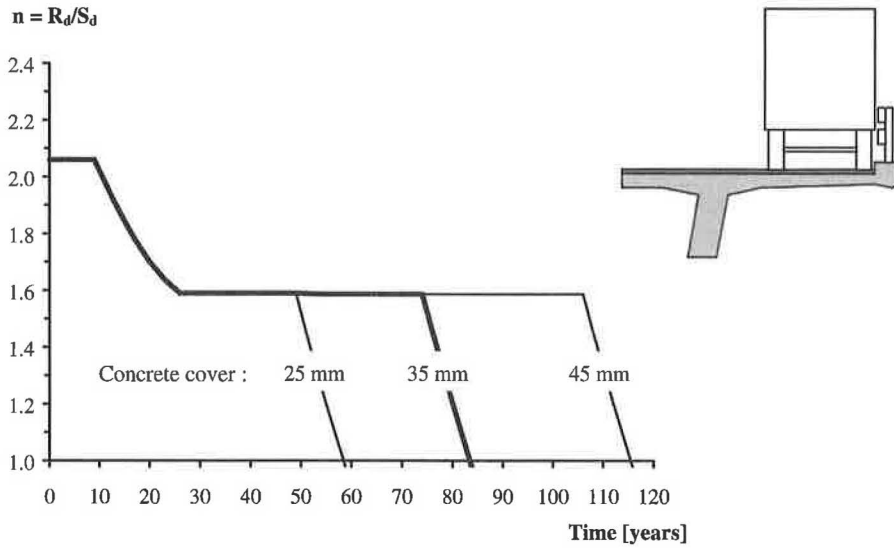
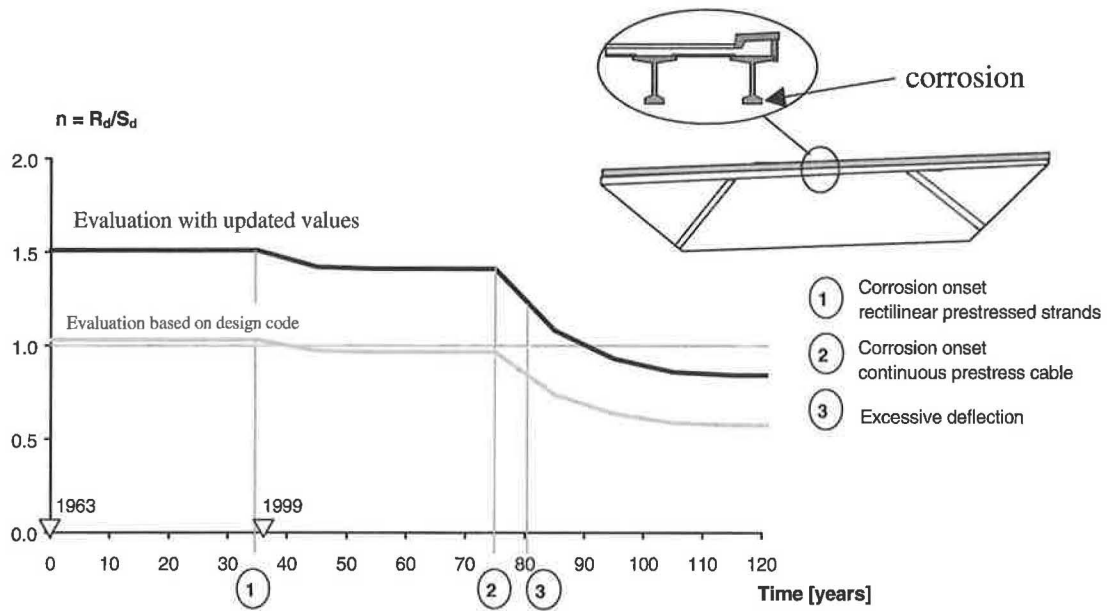*Figure 6: Local failure of the cantilever with different concrete covers.*

Figure 7: Decreasing safety coefficient with respect to time of the strut bridge.

concrete cover of 25 mm. Figure 6 shows the safety coefficient *n* with respect to time of the strut bridge.

The corrosion initiation times of the prestressed wires and the prestressed cables in the girders were calculated to be 35 years and 75 years, respectively. The start of corrosion of the prestressed wires caused the first drop in safety (Figure 7). The start of corrosion of the prestressed cables caused the second drop in safety.

The safety coefficient *n* is sufficient until the corrosion of the prestressed cables. Then the safety drops quickly and becomes insufficient after 90 years of service life. The bridge is predicted to have serviceability problems due to excessive deflections before the safety coefficient falls below acceptable limits. The deck deflection due to the dead load becomes unacceptable at 80 years.

CONCLUSIONS

This paper demonstrates the use of a segmental approach in which accurate deterioration models and non-destructive testing can be employed to predict the condition evolution of a bridge. The preliminary conclusions of this on-going research are:

- Non-destructive tests give quantitative values from which to predict the condition evolution of the bridge.
- Chloride corrosion initiation time has a larger influence on the service life of the structure than the corrosion speed of the steel.
- Deterioration curves are discontinuous. The safety coefficients have several plateaus due to multiple load paths.

In order to include this method in Bridge Management Systems, it is necessary to determine:

- Typical bridge and typical failure scenarios
- Deterioration curves for each failure scenario
- Markov chains based on a probabilistic condition evolution.

REFERENCES

1. Adey, B., Roelfstra, G., Hajdin, R., and Bruhwiler, E., *Permeability of existing concrete bridges*, Proceedings, 2nd International PhD Symposium in Civil Engineering, Budapest, 1998, pp. 110–117.

2. Torrent, R., and Frenzer, G., *Measurement methods and assessment of in situ the concrete cover properties*, Report No. 516, Union des professionnels suisses de la route (VSS), Zürich, 1995 (in German).

3. Bazant, Z.P., *Creep and shrinkage of concrete: Mathematical modeling*, Fourth RILEM International Symposium, Illinois, 1986.

4. Saetta, A.V., Scotta, R.V., and Vitaliani, R.V., *Analysis of chloride diffusion into partially saturated concrete*, ACI Materials Journal, 1993, pp. 441–451.

5. Flückiger, D., Elsener, B., and Böhni, H., *Chloride in Concrete—Transport and Assessment, Chloride im Beton: Transport und Erfassung,* Report No. 520, Union des professionnels suisses de la route (VSS), Zürich, 1996.

6. Konin, A., Francois, R., and Arliguie, G., *Penetration of chlorides in relation to the microcracking state into reinforced ordinary and high strength concrete,* Material and Structures, Vol. 31, June 1998, pp. 310–316.

7. Mangat, P. S., and Molloy, B. T., *Prediction of free chloride concentration in concrete using routine inspection data,* Magazine of Concrete Research, 46, No. 169, 1994, pp. 279–287.

8. Breit, W., *Critical corrosion inducing chloride content—State of the art (Part I),* Betontechnische Berichte, 1998(7), pp. 442–449.

9. Gonzalez, J.A., et al., *Comparison of rates of general corrosion and maximum pitting penetration on concrete embedded steel reinforcement,* Cement and Concrete Research, 25(2), pp. 257–264.

10. SIA Code 160, *Actions on structures,* and SIA Code 162, *Concrete Structures,* Swiss Society of Engineers and Architects, Zürich, 1989.